

Micropatterned Protective Membranes Inhibit Lens Epithelial Cell Migration in Posterior Capsule Opacification Model

Chelsea M. Magin¹, Rhea M. May¹, Michael C. Drinker¹, Kevin H. Cuevas², Anthony B. Brennan^{1,3}, and Shravanthi T. Reddy¹

¹Sharklet Technologies, Inc., Aurora, CO, USA

²Rocky Mountain Ophthalmology and InSight Innovations, LLC, Golden, CO, USA

³Department of Materials Science & Engineering and J. Crayton Pruitt Family Department of Biomedical Engineering, University of Florida, Gainesville, FL, USA

Correspondence: Shravanthi T. Reddy; 12635 E. Montview Blvd., Suite 155, Aurora, CO 80045; e-mail: sreddy@sharklet.com

Received: 9 December 2014

Accepted: 4 February 2015

Published: 13 March 2015

Keywords: intraocular lens; microtopography; cell migration; posterior capsule opacification; cataract surgery

Citation: Magin CM, May RM, Drinker MC, Cuevas KH, Brennan AB, Reddy ST. Micropatterned protective membranes inhibit lens epithelial cell migration in posterior capsule opacification model. *Tran Vis Sci Tech.* 2014;4(2):9, <http://tvstjournal.org/doi/full/10.1167/tvst.4.2.9>, doi:10.1167/tvst.4.2.9

Purpose: To evaluate the ability of Sharklet (SK) micropatterns to inhibit lens epithelial cell (LEC) migration. Sharklet Technologies, Inc. (STI) and InSight Innovations, LLC have proposed to develop a Sharklet-patterned protective membrane (PM) to be implanted in combination with a posterior chamber intraocular lens (IOL) to inhibit cellular migration across the posterior capsule, and thereby reduce rates of posterior capsular opacification (PCO).

Methods: A variety of STI micropatterns were evaluated versus smooth (SM) controls in a modified scratch wound assay for the ability to reduce or inhibit LEC migration. The best performing topography was selected, translated to a radial design, and applied to PM prototypes. The PM prototypes were tested in an in vitro PCO model for reduction of cell migration behind an IOL versus unpatterned prototypes and IOLs with no PM. In both assays, cell migration was analyzed with fluorescent microscopy.

Results: All SK micropatterns significantly reduced LEC migration compared with SM controls. Micropatterns that protruded from the surface reduced migration more than recessed features. The best performing micropattern reduced LEC coverage by 80%, $P = 0.0001$ (ANOVA, Tukey Test). Micropatterned PMs reduced LEC migration in a PCO model by 50%, $P = 0.0005$ (ANOVA, Tukey Test) compared with both IOLs with no PM and IOLs with SM PMs.

Conclusions: Collectively, in vitro results indicate the implantation of micropatterned PMs in combination with posterior chamber IOLs could significantly reduce rates of clinically relevant PCO. This innovative technology is a globally accessible solution to high PCO rates.

Translational Relevance: A novel IOL incorporating the SK micropattern in a membrane design surrounding the optic may help increase the success of cataract surgery by reducing secondary cataract, or PCO.

Introduction

Cataract is the leading cause of blindness and visual impairment in the world accounting for 33% and 51% of cases, respectively.¹ The World Health Organization estimates that 20 million patients worldwide currently suffer from severely reduced vision as a result of cataract.² The number of patients requiring cataract treatment is predicted to grow to 40

million by 2020, as the aged population continues to increase.² The only means to treat cataract is surgical intervention and as such cataract surgery and artificial intraocular lens (IOL) implantation is the most common procedure performed by ophthalmologists.³ Posterior capsular opacification (PCO) is the most prevalent complication of cataract surgery. Following surgical extraction of the crystalline lens, residual lens epithelial cells (LECs) rapidly proliferate and migrate behind the newly implanted intraocular

lens (IOL). As LECs encroach on the visual axis and opacify the posterior lens capsule, secondary loss of vision occurs in up to 50% of the patients that undergo cataract surgery each year.^{4,5}

At present, Nd:YAG laser capsulotomy follow-up surgery is implemented to correct this secondary visual impairment. Although these follow-up procedures are relatively quick and easy to perform, complications including retinal detachment, damage to the IOL, elevated intraocular pressure, and vitreous floaters can occur.⁶ Laser capsulotomy procedures represent a considerable burden to national health care systems. Annual Medicare costs in the United States for laser capsulotomy procedures are currently \$280 million and the burden is expected to exceed \$1 billion by 2050.⁷

Treating cataract and secondary vision loss due to PCO in developing countries is a formidable challenge magnified by both higher rates of cataract in these areas and the fact that laser treatment is not readily available.^{2,6,8} It is estimated that over 90% of the world's visually impaired are living in developing countries with limited access to treatment for causes of avoidable blindness.¹ In India, for example, age-adjusted prevalence of cataract is three times that of the United States.² Nd:YAG laser capsulotomy is so rarely available in these areas that in a study, which included four developing countries, less than 1% of patients with visually impairing PCO received treatment.² When laser capsulotomy is available, treatment in developing countries is often less effective with more frequent complications.⁶ Better control of the pathogenic mechanism of PCO is therefore highly desirable as a basis for improving the outcome of cataract surgery and eradicating PCO worldwide.

A globally accessible alternative strategy for reducing PCO rates involves redesigning the ophthalmic devices that are implanted. Progress in IOL design shows that hydrophobic materials reduce LEC attachment and therefore PCO rates more than hydrophilic materials.⁹ Additionally, IOLs, designed with sharp corners at the optic edge, form a physical barrier to cell migration, and reduce but do not eliminate PCO.¹⁰⁻¹³ Although incidence of PCO has decreased since the introduction of sharp-edge IOLs in clinical practice, clinical studies have shown that LECs migrated across the sharp edge of the IOL optic in 58% of cases, preferentially at the optic-haptic junction in both one- and three-piece IOL designs.^{10,14} Recently, a disc-shaped haptic design has emerged as an innovative alternative to these traditional IOL designs. The Anew Zephyr open-bag IOL

has been shown to reduce development of PCO in both an in vitro organ culture model¹⁵ and an in vivo rabbit model.¹⁶ Even though this new IOL design reduced PCO compared with traditional square-edge designs, the posterior component of the haptic ring is smooth and it is possible that a squared edge could further improve resistance to PCO.¹⁵ A novel concept presented here is to use a Sharklet patterned protective membrane (PM) implanted in combination with a posterior chamber IOL. The device, which combines both square-edged haptic ring and micropattern technologies, should inhibit cellular migration across the posterior capsule.

Cells migrate through the interaction of focal adhesions, protein assemblies embedded in the cell membrane, with biomaterial interfaces.¹⁷ Micropatterns act to control cell migration by directing the placement of focal adhesions.^{18,19} The unique discontinuous features that comprise the Sharklet micropattern allow for focal adhesions to be precisely guided, and therefore provide a high level of control over the migration orientation for a cell population. It was thus hypothesized that Sharklet micropatterns could be optimized to inhibit LEC migration.

To determine the feasibility of this approach, several microtopographies were tested in a modified scratch-wound test to assess LEC migration. The best performing pattern was then applied to a PM prototype and tested in an in vitro PCO model to evaluate the influence of a micropatterned PM on LEC migration. Results were compared with an unpatterned membrane and an IOL without a PM. The micropatterned PMs have design features, such as a hydrophobic base material, a peripheral square edge and a micropattern that inhibit cell migration in all directions.

Materials and Methods

Sample Fabrication

Smooth and micropatterned samples were fabricated by casting biomedical grade polydimethylsiloxane elastomer (PDMS_e, Silastic MDX4-4210; Dow Corning, Midland, MI) against negative silicon wafer molds. The micropatterns produced by this technique were comprised of discontinuous channel features arranged in a SK pattern that either protruded (+) from or were recessed (-) into the PDMS_e surface. Using the current nomenclature a pattern with features protruding 3 μm from the surface that were 2-μm wide and spaced by 2 μm would be called

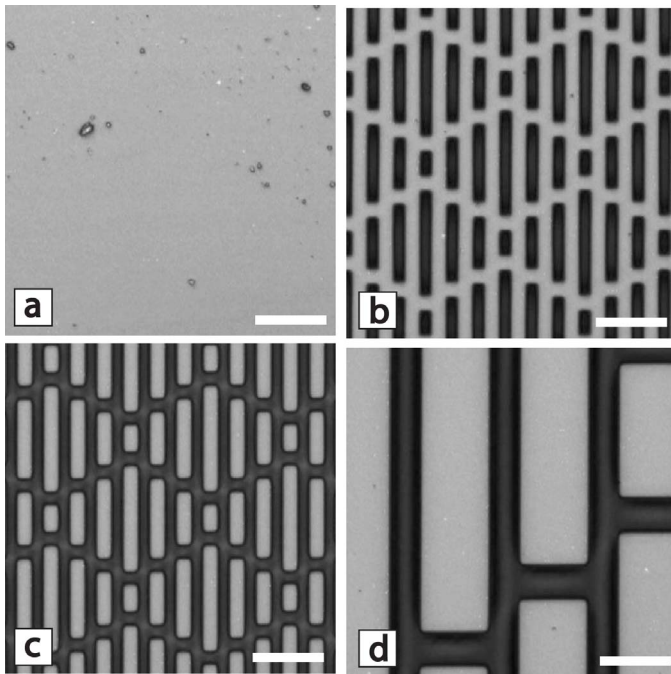


Figure 1. Confocal microscopy images of (a) SM, (b) -3SK2x2, (c) +3SK2x2, and (d) +7SK10x5 Sharklet micropatterns replicated in biomedical grade PDMS_e. Scale bars: 10 µm.

+3SK2x2. The micropatterns replicated for testing included SM, -3SK2x2, +3SK2x2, and +7SK10x5 (Fig. 1).

LEC Migration Assay

Circular samples (diameter = 20 mm) were adhered to a 12-well plate with features aligned perpendicular to the direction of cell migration and treated with 15 µg/mL fibronectin (BD Biosciences, San Jose, CA) in phosphate buffered saline (Life Technologies, Carlsbad, CA) overnight to facilitate cell attachment. A modified scratch-wound assay²⁰ (Fig. 2) was created by blocking cell attachment to the samples using SM PDMS_e rectangles (3 mm × 20 mm) placed along the center of the sample (Fig. 2a). LECs (ATCC CRL-11421; ATCC, Manassas, VA) were seeded over the entire configuration at 1×10^4 cells/cm² and maintained in growth media (Eagle's minimum essential media; ATCC), 20% fetal bovine serum (Life Technologies), 50 U/mL penicillin/streptomycin (Life Technologies), and 1 µg/mL Fungizone antimycotic (Life Technologies; Fig. 2b).

When LECs reached approximately 70% confluence, PDMS_e rectangles were removed to allow cell migration across the empty patterned or unpatterned area, which simulates the wound area (Fig. 2c). Migration was monitored via light microscopy until

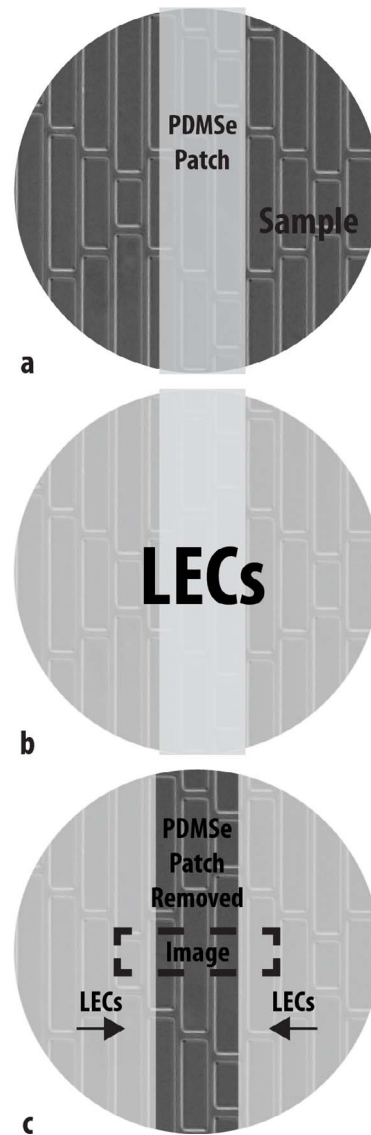


Figure 2. Schematic of the LEC migration assay procedure. (a) Samples were arranged perpendicular to the direction of cell migration and a rectangular PDMS_e patch was placed across each sample to block cell adhesion to that area. (b) Cells were seeded onto the entire surface and allowed to grow to approximately 70% confluence. (c) PDMS_e patches were removed and cell migration into the artificial wound was monitored.

Day 7 when samples were stained with CellTracker Orange CMTMR (Life Technologies) according to the manufacturer's instructions and fixed with 4% paraformaldehyde (Electron Microscopy Sciences, Hatfield, PA) for 15 minutes at room temperature. Fluorescent microscopy images were taken of the wounded area and the average area covered by cells within this region was calculated using ImageJ software (National Institutes of Health, Bethesda,

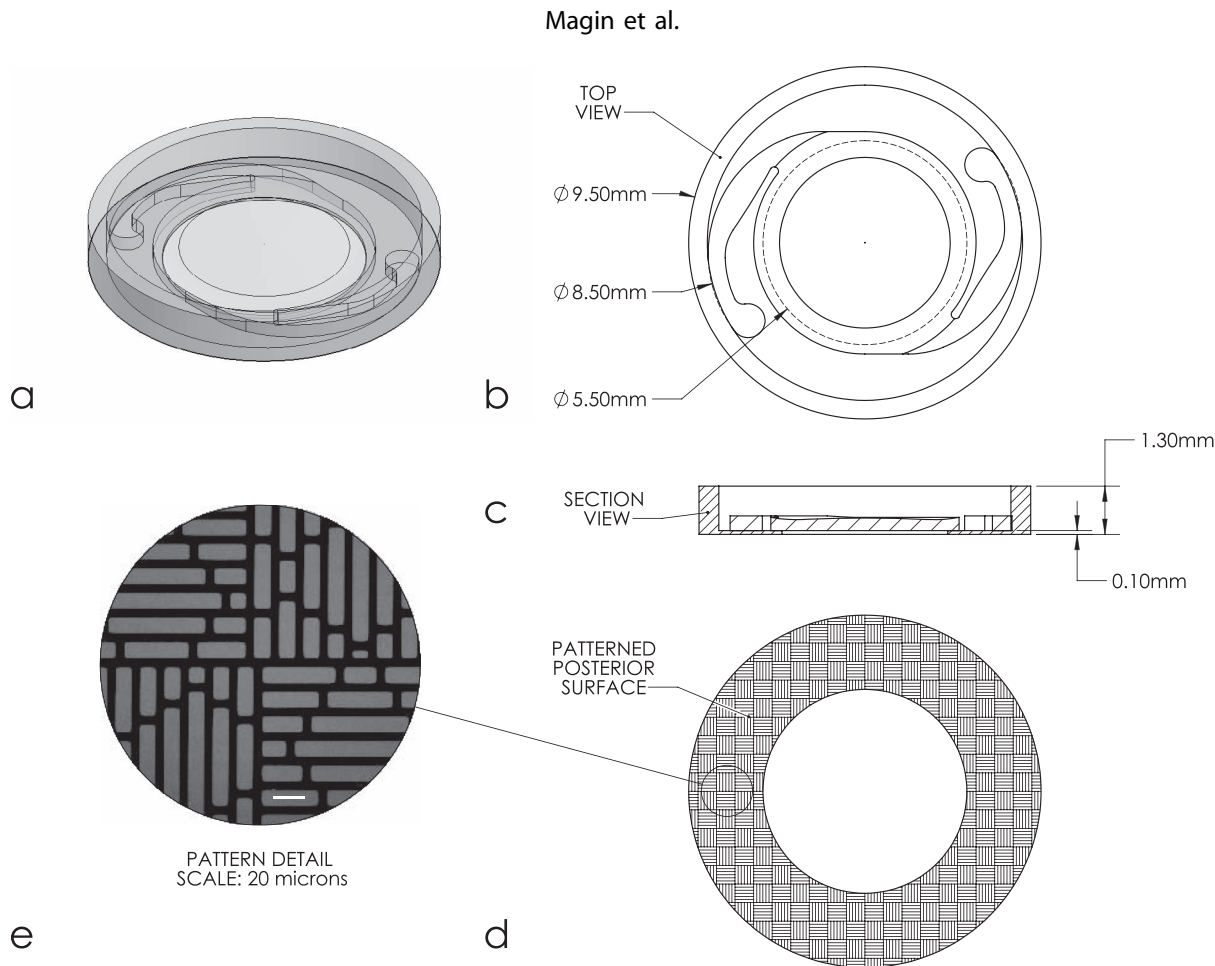


Figure 3. (a) A three-dimensional rendering that depicts an IOL inside a Sharklet-patterned PM. (b) A top down view of the IOL inside a PM, (c) section view of the IOL inside a PM, and (d) posterior view of the PM. (e) The checkerboard pattern shown in the confocal micrograph covers the posterior side of the PM. Scale bar: 20 μm .

MD). Experiments were performed in triplicate with $n = 3$ replicates.

PM Prototype Design and Production

Prototypes were designed with a square-edge haptic ring (outer diameter = 9.5 mm) that fits the natural curvature of the lens capsule and provides a ridge (height = 1.2 mm) to engage and retain IOL haptic arms. A thin membrane (thickness = 0.1 mm) spanned the area between the haptic ring and an aperture for the IOL optic (diameter = 5.5 mm). This membrane was designed to rest against the posterior capsule to inhibit cell migration from the periphery of the lens capsule (Fig. 3). The posterior surface of the PM was unpatterned (negative control) or patterned with the best performing pattern identified in migration assays. The micropattern was tiled to create a checkerboard pattern with alternating orientation of the pattern in each 500- μm square to produce a

surface that blocks LEC migration from all directions (Fig. 3). Steel casting molds were designed and machined by 10 \times MicroStructures (Wheeling, IL) for PM prototype production. PM prototypes were replicated in PDMSe and sterilized by immersion in 70% ethanol in water (vol/vol) prior to use.

PCO Model

An in vitro model to simulate the formation of PCO after cataract surgery²¹ was constructed as previously described. Briefly, an IOL with or without a PM was placed into a 6-well plate containing a collagen-coated transwell insert (Corning, Corning, NY). Each assay evaluated IOLs (AcrySof IQ TORIC; Alcon, Minitab, Inc., Fort Worth, TX) without a PM, IOLs combined with unpatterned PMs and IOLs combined with Sharklet-patterned PMs. A silicone washer was placed around the outside of the well to either engage the haptics of the IOL or

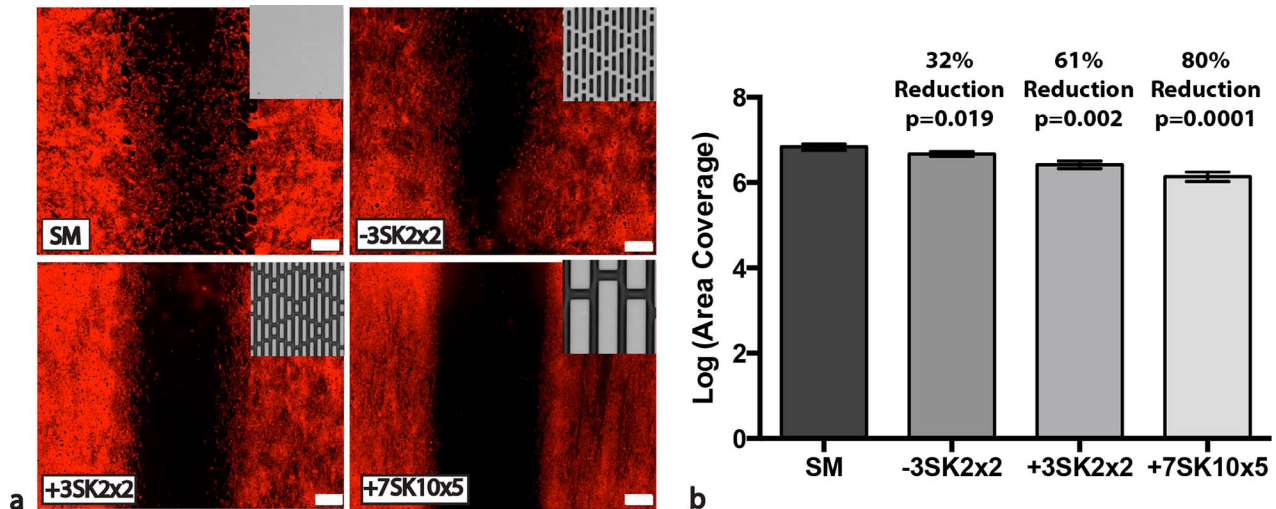


Figure 4. (a) Representative fluorescent images of cells stained with CellTracker (red) on PDMS samples at the migration assay endpoint (7 days). Scale bars: 500 μm . (b) Average, transformed coverage of wounded area by cells in migration assays at the 7-day time point. Error bars: 95% confidence intervals. All Sharklet micropatterns reduced cell migration into the wounded area compared with SM (ANOVA, Tukey Test). The +7SK10x5 exhibited the highest reduction in cell migration (80% compared with SM).

to establish the same surface area available for cell attachment around all IOLs and IOL/PM combinations. The entire assembly was weighted down (~ 5 g) to ensure that IOLs maintained contact with the collagen membranes.

LECs were seeded into each well at 1×10^4 cells/ cm^2 and maintained in growth media (Eagle's minimum essential media, 20% fetal bovine serum, 50 U/mL penicillin/streptomycin, and 1 $\mu\text{g}/\text{mL}$ Fungizone antimycotic). After 7 days, cells were stained with CellTracker Orange CMTMR (Life Technologies) according to the manufacturer's instructions and fixed with 4% paraformaldehyde (Electron Microscopy Sciences, Hatfield, PA) for 15 minutes at room temperature. Fluorescent microscopy was used to focus on cells attached to the collagen membrane both outside and behind each sample, images were taken of each sample type, and the average surface area coverage behind the IOL was calculated using ImageJ software for $n = 3$ replicates in three experiments.

Statistical Analysis

Area coverage (A) measurements were normalized via logarithmic transformation for migration assays. Log reductions were calculated for each experiment by subtracting the average log ($A_{\text{micropattern}}$) from the average log (A_{smooth}). Normality of each data set was confirmed by residual and normal probability plots. The mean log reduction was converted to the median percent reduction using the equation: $1 - 10^{(-LR)}$.

Reductions from at least three experiments were compared with the null hypothesis of zero reduction by a one-sided t -test to determine statistical significance. Estimates of the among- and within-experiment variances were assessed using analysis of variance (ANOVA) of the log transformed area coverage values for each SM and micropatterned sample, with a random effect for experiment.

PCO model data were also normalized via logarithmic transformation. Normality of each data set was confirmed by residual and normal probability plots. Data from three experiments were pooled after confirming equal variances ($P = 0.529$; Levene's Test) and compared using ANOVA and Tukey Test for multiple comparisons. All analyses were performed using MiniTab16 statistical software (State College, PA).

Results

Migration Assay

All Sharklet topographies significantly reduced LEC migration compared with SM (Fig. 4). Micropatterns that protruded from the surface reduced migration more than recessed features. Each pattern grouped separately in a Tukey Test for multiple comparisons indicating that all patterns had significantly different levels of performance. The best performing surface, +7SK10x5, reduced LEC coverage in the wounded area by 80% ($P = 0.0001$;

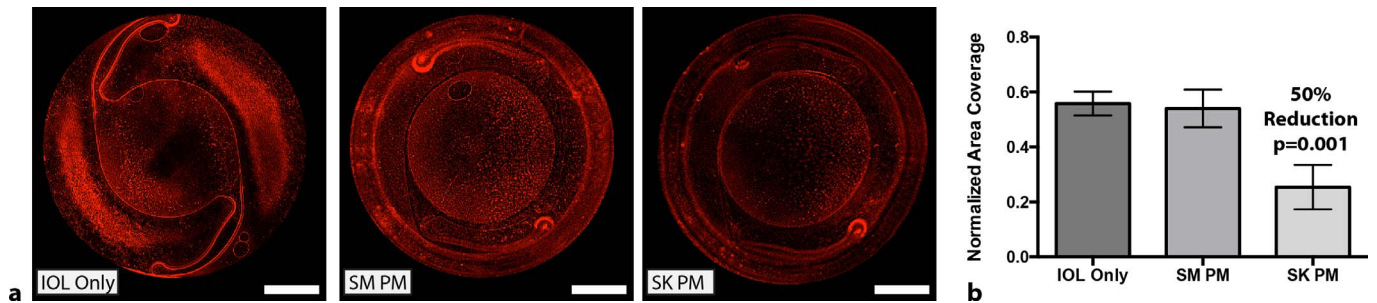


Figure 5. (a) Representative fluorescent images of LECs stained with CellTracker (red) at the PCO model assay endpoint (7 days). Scale bars: 2 mm. (b) Average log transformed area coverage within the IOL optic in PCO model assays at the 7-day time point. Sharklet-patterned PMs reduced cell coverage by 50% (ANOVA, Tukey Test) compared with IOL Only and SM PMs. Error bars: 95% confidence intervals.

ANOVA, Tukey Test). Based on these results, the +7SK10x5 pattern was selected for arrangement into a checkerboard design intended to inhibit LEC migration from all directions and applied to PMs for additional testing.

PCO Model

Prototype PMs with a square-edge haptic ring and a thin membrane modified with the checkerboard +7SK10x5 pattern reduced LEC migration between the collagen membrane and the IOL by 50% ($P = 0.0005$; ANOVA, Tukey Test) compared with the IOL only condition (Fig. 5). PMs with SM membranes did not significantly reduce LEC migration compared with the IOL only condition. These results confirm that the +7SK10x5 Sharklet pattern controls cell migration in all directions when tiled into a checkerboard arrangement.

Discussion

Innovative approaches to altering IOLs have reduced PCO rates in animal models¹⁶ but remain inaccessible to the global community due to the high cost of cutting-edge technology. An inexpensive device capable of preventing PCO that could be used in conjunction with existing IOL devices would improve patient care by eliminating the need for laser capsulotomy, substantially reducing associated risks and costs. Collectively, our results show that the micropattern disrupts the pathogenic mechanism of PCO by inhibiting cellular migration across the visual axis.

We have demonstrated in this study the ability to control integrin-mediated cell migration using Sharklet micropatterned surface technology. Micro- and nanoscale patterns have previously been shown to control ocular cell migration by directing placement

of focal adhesions.^{18,22} The majority of these studies attempted to recapitulate the native morphology of ocular tissue. This strategy has demonstrated that parallel ridge topographies with heights up to 1.6 μm induced alignment and directed migration of ocular cells.^{19,23} Micropatterns with heights above this threshold predominately induced migration along the groove direction and subsequently reduced migration rates significantly compared with those of cells on ridges with nanoscale heights.²³ The results of this study are consistent with these findings. All Sharklet micropatterns reduced LEC migration in a modified scratch-wound assay. Features that protruded from the surface reduced migration more than features that were recessed into the surface. Additionally, the +7SK10x5 Sharklet micropattern significantly outperformed the shorter +3SK2x2 pattern, 80% versus 61% reduction.

Due to the circular nature of the ocular capsular bag, it was essential to develop a pattern to block cell migration from all directions. The +7SK10x5 micropattern was arranged so that micropattern orientation alternated every 500 μm to block LEC migration radially. Results from an in vitro PCO model indicated that the +7SK10x5 checkerboard-patterned PMs reduced migration between a collagen membrane and an IOL by 50% ($P = 0.001$; ANOVA, Tukey Test) compared with the IOL only condition. These results confirm that the new pattern configuration does reduce cell migration in a circular environment. Although this in vitro model cannot replicate the bending of the capsular bag that occurs in vivo, correctly sizing the device will result in a tight capsular bend in the peripheral bag at the square edge.¹² This stretching of the posterior capsule should eliminate space between the capsule and the PM and in turn present both the square edge¹² and the Sharklet-patterned PM as mechanical barriers to

LEC migration. To validate these results, PMs will be tested in an established rabbit model for PCO.¹⁶

Collectively, these results indicate that the implantation of an inexpensive micropatterned PM in combination with a posterior chamber IOLs could significantly reduce rates of clinically relevant PCO in developing countries. This innovative technology may provide a globally accessible solution to high PCO rates and thus high levels of visual impairment in developing countries.

Acknowledgments

The authors thank B.C. Stevenson for fabricating, imaging, and characterizing micropatterned samples and M.R. Mettetal for producing Figure 3.

Supported by grants from the National Institutes of Health (NIH) National Eye Institute SBIR Phase I Grant Number: 1R43EY022541-01A1.

References

- World Health Organization. Global Data on Visual Impairments 2010. 2012. www.who.int, Accessed July 23, 2014.
- Brian G, Taylor H. Cataract blindness: challenges for the 21st century. *Bull World Health Org.* 2001; 79:249–256.
- Wormstone MI. Posterior capsule opacification: a cell biological perspective. *Exp Eye Res.* 2002; 74:337–347.
- Schaumberg DA, Dana MR, Christen WG, Glynn RJ. A systematic overview of the incidence of posterior capsule opacification. *Ophthalmology.* 1998;105:1213–1221.
- Marcantonio JM, Vrensen GFJM. Cell biology of posterior capsular opacification. *Eye.* 1999;13: 484–488.
- Awasthi N, Guo S, Wagner BJ. Posterior capsular opacification: a problem reduced but not yet eradicated. *Arch Ophthalmol.* 2009;127: 555–562.
- Medicare. *Medicare Payments and Frequency for Cataract Surgery YAG Capsulotomy, Medicare PSPS Data for 2009.* Corcoran Consulting Group; 2009.
- Tabin G, Chen M, Espandar L. Cataract surgery for the developing world. *Curr Opin Ophthalmol.* 2008;19:55–59. 10.1097/ICU.1090b1013e3282f1154bd.
- Cooke CA, McGimpsey S, Mahon G, Best RM. An in vitro study of human lens epithelial cell adhesion to intraocular lenses with and without a fibronectin coating. *Invest Ophthalmol Vis Sci.* 2006;47:2985–2989.
- Nixon DR, Apple DJ. Evaluation of lens epithelial cell migration in vivo at the haptic-optic junction of a one-piece hydrophobic acrylic intraocular lens. *Am J Ophthalmol.* 2006;142:557–562.
- Nagamoto T, Fujiwara T. Inhibition of lens epithelial cell migration at the intraocular lens optic edge: role of capsule bending and contact pressure. *J Cataract Refract Surg.* 2003;29:1605–1612.
- Nishi O, Yamamoto N, Nishi K, Nishi Y. Contact inhibition of migrating lens epithelial cells at the capsular bend created by a sharp-edged intraocular lens after cataract surgery. *J Cataract Refract Surg.* 2007;33:1065–1070.
- Packer M, Rajan M, Ligabue E, Heiner P. Clinical properties of a novel, glistening-free, single-piece hydrophobic acrylic IOL. *Clin Ophthalmol.* 2014;8:421–427.
- Findl O, Hirsenschall N, Nishi Y, Maurino V, Crnej A. Capsular bag performance of a hydrophobic acrylic 1-piece intraocular lens. *J Cataract Refract Surg.* 2015;41:90–97.
- Eldred JA, Spalton D, Wormstone IM. An in vitro evaluation of the Anew Zephyr® open bag IOL in the prevention of posterior capsule opacification using a human capsular bag model. *Invest Ophthalmol Vis Sci.* 2014;55:7057–7064.
- Kavoussi SC, Werner L, Fuller SR, et al. Prevention of capsular bag opacification with a new hydrophilic acrylic disk-shaped intraocular lens. *J Cataract Refract Surg.* 2011;37:2194–2200.
- Huttenlocher A, Horwitz AR. Integrins in cell migration. *Cold Spring Harb Perspect Biol.* 2011; 3:a005704.
- Xia N, Thodeti CK, Hunt TP, et al. Directional control of cell motility through focal adhesion positioning and spatial control of Rac activation. *FASEB J.* 2008;22.
- Rajnicek AM, Foubister LE, McCaig CD. Alignment of corneal and lens epithelial cells by co-operative effects of substratum topography and DC electric fields. *Biomaterials.* 2008;29: 2082–2095.
- Marmaras A, Lendenmann T, Civenni G, et al. Topography-mediated apical guidance in epidermal wound healing. *Soft Matter.* 2012;8:6922–6930.
- Gotoh N, Perdue NR, Matsushima H, Sage EH, Yan Q, Clark JI. An in vitro model of posterior

- capsular opacity: SPARC and TGF- β 2 minimize epithelial-to-mesenchymal transition in lens epithelium. *Invest Ophthalmol Vis Sci.* 2007;48:4679–4687.
22. McHugh KJ, Saint-Geniez M, Tao SL. Topographical control of ocular cell types for tissue engineering. *J Biomed Mater Res B Appl Biomater.* 2013;101:1571–1584.
23. Diehl KA, Foley JD, Nealey PF, Murphy CJ. Nanoscale topography modulates corneal epithelial cell migration. *J Biomed Mater Res A.* 2005;75A:603–611.